Universiteit Utrecht

Faculteit Bètawetenschappen

Growth Process of Disk- and Rod- Shaped Bacterial Colonies in 2D

Bachelor Thesis

Corné Wiggers

Natuur- en Sterrenkunde

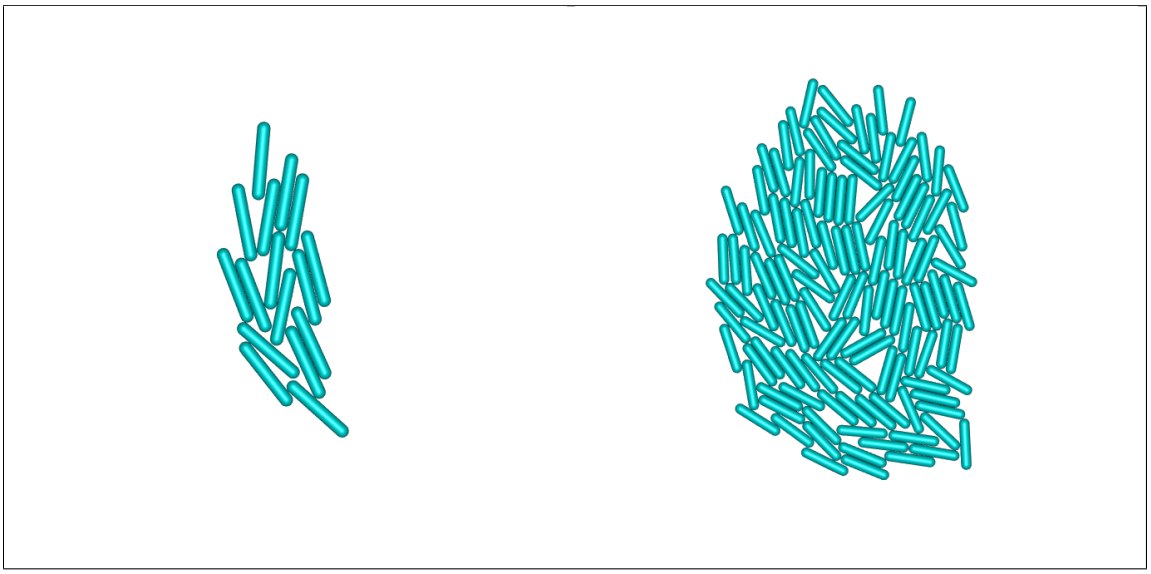

Supervisors:

Dr. Joost de Graaf Supervisor
Institute for Theoretical Physics

Meike Bos Daily Supervisor
Institute for Theoretical Physics

June 11, 2020

Abstract

Bacterial colonies play an important role in the global ecosystem, but the mechanical interactions between bacteria are not always well understood. In this thesis, we investigated the role of the aspect ratio (e.g. disk- and rod shaped bacteria) and the ratio between diffusion and duplication rate on the size and shape of a bacterial colony. We simulated growing bacterial colonies of particles with different aspect ratios in 2D using Brownian dynamics. The simulated colonies are analysed by looking at their mean radius, shape and the nematic order parameter. We find that for all the simulations the mean radius grows exponentially in time. For the rod-shaped bacterial colonies we find that the system starts in an elliptical nematic state that converges in time slowly to a circular isotropic state, due to outward radial pressure and the creation of disorder. The disk-shaped bacterial colonies with a fixed duplication direction start as well with an elliptical shape that converges to a circular shape. For a growing disk-shaped bacterial colony with a random duplication direction, we always find a circular shape. Moreover, we find that a higher diffusion rate leads to a higher mean radius of a bacterial colony on a short timescale but on a longer timescale the diffusion rate does not affect the mean radius due to the dominancy of the duplication rate. In future research it would be interesting to look at polydisperse colonies consisting of bacteria with different aspect ratios.

Contents

1 Introduction

In the world many systems are composed of active matter [1]. Active matter consists of particles that can consume energy to create motion or perform other kinds of work (such as division). A popular example of an active matter system is a flock of birds [2]. Birds can add energy to the system by subtracting energy out of the food they eat and use this energy to accelerate in some specific direction. Due to this the system will never reach an equilibrium. Furthermore, birds will tend to align themselves with their nearest neighbours. A growing colony consisting of nonmotile bacteria is also active matter. Nonmotile means that the bacteria are incapable of self-propelled movement and that all the movements inside the colony are created by collisions with other particles and by thermal fluctuations. Just like birds these bacteria consume food and convert this into motion. However, the way they create this motion is different, because unlike nonmotile bacteria, birds move by a self-propelled motion. Nonmotile bacteria create motion by interactions with other bacteria. At a low density the bacteria communicate mainly through chemical signals [3]. However, at a high density mechanical interactions between the bacteria dominate the dynamics of the system [4]. As the bacteria keep growing, they push their neighbouring bacteria away and therefore a motion is produced. Furthermore, bacteria will tend to orientate themselves in the same direction as their neighbours. However, due to local energy input misalignments are actively created. Understanding the mechanics behind a growing bacterial colony has advantages in practical fields such as food safety [5].

In this thesis, we investigated the role of the aspect ratio and the ratio between diffusion and duplication rate on the size and shape of a bacterial colony. Moreover, we looked how the alignment of the bacteria affects the growth process. Therefore we simulated a bacterial colony of rod-shaped particles. However, to get a good understanding of the effect of aligned particles in a colony, we first studied the properties of a colony without nematic structures. Therefore we used disk-shaped bacteria. Afterwards we compared the two different bacterial colonies to find the effect of the formation of alignments on the growth process.

We simulated the physical processes of a growing bacterial colony using Brownian dynamics. We used Brownian dynamics, because for bacteria viscous forces dominate and therefore inertial effects can be ignored. This is due to the small sizes of bacteria (a diameter in the order of a few micrometers). The simulations are done for both the disk- and rod-shaped bacteria. Three different methods are used to analyse the growing colonies. These are the mean radius, the shape of the colony and the orientation of the bacteria. The latter is only used for rods as disks do not have orientational order. Moreover, simulations are compared for different diffusion duplication ratios, a different duplication direction for the disk-shaped bacteria and different aspect ratios for the rod-shaped bacteria. This is explained in more detail in the next chapter.

We found for disk-shaped particles that for a random duplication direction they grow exponentially and that the shape of the colony is circular. On a longer timescale we found the same results for a fixed duplication direction, however on a short timescale this system will have a slightly higher growth rate and an elliptical shape. For rod-shaped bacteria, the results are similar to that of disk-shaped bacteria with a fixed duplication direction. Thus on the short timescale an exponential growth rate, an elliptical shape and moreover the rods will be aligned in a nematic structure. On a longer timescale the shape of the system enters an isotropic circular state. This is a result of the misalignment that is created, due to thermal fluctuations. Although the global state is now isotropic, we still found many small local nematic regions in the colony. Furthermore, we concluded that increasing the diffusion rate increases the mean radius of the

colony on a short time scale, however on a longer time scale the mean radius of the system looks the same as that of systems with different diffusion rates, due to the increasing dominancy of the duplication rate over time. In further research we suggest to look to the growth process of a colony consisting of different shaped particles.

This thesis is organized as follows. In chapter 2, the implementation of the Brownian Dynamics simulation is explained. Followed by the implementation of disk- and rod-shaped bacteria and a short description of the used analysis methods. In chapter 3, our model is validated by comparing it with Monte Carlo simulations. Chapter 4 gives specification of the parameters that are used. In chapter 5, the simulations of the different bacterial colonies are presented and discussed. In chapter 6, a discussion is given of the model, the results and the assumptions that were made in this thesis. Chapter 7 concludes and gives some suggestions for further research.

2 Methodology

In this chapter, we explain the simulation methods that have been used in this thesis. A lot of bacteria have approximately the shape of a disk or that of a rod. For example, the Neisseria bacteria are disk-shaped and can be found in the mucosal surfaces of many animals [6]. And an example of rod-shaped bacteria is the Escherichia coli, that can be found in your intestines [7]. In this thesis we used Brownian dynamics simulations of interacting disk- and rod-shaped particles to simulate the behaviour of bacterial colonies.
Firstly, this chapter gives an explanation of Brownian dynamics. Secondly, we explain the two different interaction potentials that are used in this thesis. These are the Hertzian potential and the spring potential. Thirdly, we describe how the disk- and rod-shaped bacteria have been implemented. This includes how the bacteria are defined, how they interact and how they duplicate themselves. Finally, this chapter gives a discussion of the different analysing methods that have been used to study the bacterial colonies.

2.1 Brownian Dynamics

For a bacterial system in a liquid the Reynolds number, which is given by $Re = \frac{\text{inertial forces}}{\text{drag forces}}$, is much smaller than one. This is due to the small sizes of the bacterial cells, they have a diameter in the order of a few micrometers. This is known as Stokes regime, where viscous forces dominate and therefore inertial effects can be ignored. This is called an overdamped system. In this overdamped system the motion can be described by Brownian dynamics. In this model the particles move by forces that are derived every time step and are then integrated. In our model we consider three forces, namely the drag force, the thermal force and the interaction force. The drag force $\mathbf{F}_{\text{drag}}$ tries to slow down the motion of the particles. This drag force is due to Stokes' friction, that is the friction that a spherical object with a small Reynolds number experiences in a viscous fluid. Stokes' friction is given by $\mathbf{F}_{\text{drag}} = -\gamma\dot{\mathbf{x}}$, where γ is the friction coefficient and $\dot{\mathbf{x}}$ is the velocity vector of the particle. Secondly, a thermal force $\mathbf{F}_{\text{thermal}}$ is included that acts like a random force due to collisions with solvent molecules in the system. The average kinetic energy of these solvent molecules does depend on the temperature of the system. The formula of this force is given by $\mathbf{F}_{\text{thermal}} = \sqrt{2\gamma k_b T}\mathbf{R}$. Here k_b is the Boltzmann constant and T is the temperature of the system and is kept fixed during the whole simulation. $\mathbf{R}$ is a vector with a random length drawn from a Gaussian distribution with mean equal to zero and a standard deviation equal to one. Finally, there is an interaction force $\mathbf{F}_{\text{int}}$ due to the interaction between the particles. The interaction forces between the particles can be calculated by taking the derivative of the potential energy, $\mathbf{F}_{\text{int}} = -\frac{dU}{d\mathbf{r}}$. Considering these three forces and ignoring inertia effects the overdamped Brownian dynamics equation of motion reads

$$\gamma\dot{\mathbf{x}} = \sqrt{2\gamma k_b T}\mathbf{R} + \mathbf{F}_{\text{int}}. \tag{2.1}$$

Unfortunately, we cannot solve this integral exactly due to the random variable $\mathbf{R}$. We solve this by switching to expectation values. Using Euler's method in the discretized form for a stochastic variable, this will lead to the following formula for the new positions of the particles

$$\mathbf{x}_{t+\Delta t} = \mathbf{x}_t + \sqrt{\frac{2k_bT}{\gamma}(\Delta t)}\mathbf{R} + \frac{\mathbf{F}_{\text{int}}}{\gamma}\Delta t. \tag{2.2}$$

Here $\mathbf{x}_t$ is the position of the particle at time step t and the term $\sqrt{\Delta t}$ follows from the width of the Gaussian distribution of these positions due to the random variable.

2.1.1 Cell Lists

With the methods described above we can simulate a bacterial colony. However, to get accurate and realistic results the simulations are often done with a total particle number N of more than thousand. To calculate all the pair-wise interaction forces this means that we have to loop over N^2 particles, which is computationally expensive. To speed up the simulation we will use cell lists. The reason for using cell lists is that the interaction force between particles is only non-zero as long as the distance between particles i and j $r^{ij} < \sigma$, where σ is a small number compared to the total system size. So instead of checking the interaction forces with all the other particles it is actually only needed to check the interaction force with the neighbouring particles that are on a distance smaller than σ. We have implemented the cell lists by dividing the simulation box into square- shaped cells with sizes slightly larger than σ. For disk-shaped particles this is visualised in figure 1.

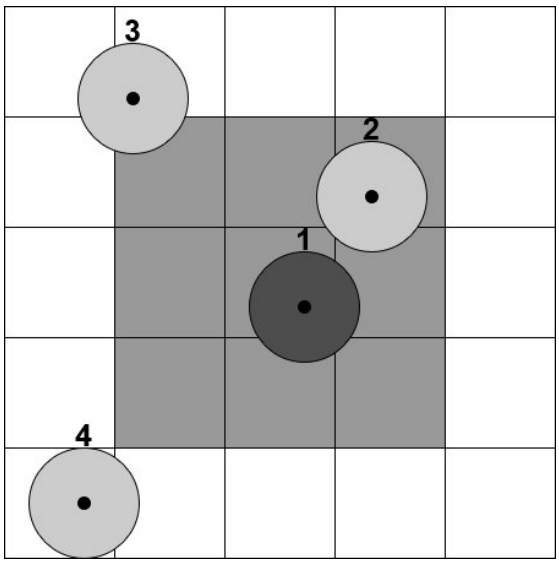

Figure 1: A visualisation of the use of cell lists for the interaction forces on particle one. Instead of checking for all the particles, we just check the particles that are placed in the grey cells.

In the simulations we now keep track in which cell these particles are located and we only loop over all the particles in the neighbouring cells to calculate the interaction force instead of looping over all the particles in the system. For example, if we look at particle one in figure 1 the centre of mass of the particle is placed in row three and column three. This means that we just have to loop over the particles that are placed in the cells that have a grey color. We only find particle two and so we only calculate the force due to this particle. Particles three and four are placed outside the grey cells and are not taken into account. This method reduces the simulation time significantly.

2.2 Potentials

Bacteria deform under pressure. To take this into account, two different soft potentials are used in the simulations. These are the Hertzian potential and the spring potential. The Hertzian

potential is used to validate the implementation of the Browninan dynamics simulation. The spring potential is used for the simulations of the bacterial colonies.

2.2.1 Hertzian potential

The Hertzian potential is implemented in a similar way as in Fomin et al.[8]. This potential has the following form

$$U_{\mathrm{h}}^{ij} = \begin{cases} \epsilon \left(1 - \dfrac{r^{ij}}{D}\right)^{\frac{5}{2}} & \text{if } r^{ij} \leq D \\ 0, & \text{otherwise} \end{cases}$$

where D is the diameter, which is used as a length scale of the system. ϵ is the energy scale and r^{ij} the distance between particle i and j. This means that the potential energy is only nonzero when particles start to overlap. The potential has a maximum value of ϵ and the potential decreases with a power of $5/2$ to zero.

2.2.2 Spring potential

For the spring potential we implemented the same potential as is used in Nordemann et al.[9]. This potential follows from Hooke's law and is given by

$$U_{\mathrm{s}}^{ij} = \begin{cases} -k_{\mathrm{s}} \left(L_{\mathrm{s}}^{\mathrm{rest}} - r^{ij}\right)^2 & r^{ij} \leq L_{\mathrm{s}}^{\mathrm{rest}} \\ 0, & \text{otherwise,} \end{cases}$$

where k_{s} is the spring constant and $L_{\mathrm{s}}^{\mathrm{rest}}$ is the rest length of the spring. This potential increases quadratically with the overlapping distance and is zero if the particles do not overlap.

2.3 Implementation of the Bacteria

In this thesis, we studied disk- and rod-shaped bacterial colonies that grow in time. Here we discuss how we have defined the bacteria in our model. Furthermore, we clarify how they interact and duplicate in time.

2.3.1 Disk- and rod-shaped particles

In this thesis a disk-shaped particle is implemented just as a disk with a diameter D. A schematic picture of such a disk can be seen in figure 2. The position of such a bacteria is given by the point in the middle of the disk.

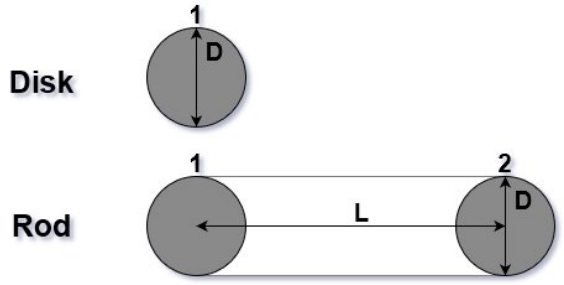

Figure 2: Schematic of a disk-shaped bacteria (top) and rod-shaped bacteria (bottom).

This thesis used the definition of rod-shaped particles as is introduced in [10] and in more detail is described in [9]. In the latter one a rod particle is formed by connecting two disks with an internal spring that has an equilibrium length L^{rest}. This can be seen in the bottom sketch of figure 2. This spring is in equilibrium when $L = L^{\text{rest}}$, where L the length of the vector $\mathbf{L}$. Here $\mathbf{L}$ is a vector that points from the centre of mass of one of the two disks in the rod to the centre of mass to the other disk and is given by

$$\mathbf{L} = \mathbf{r}_j - \mathbf{r}_i. \tag{2.3}$$

When the spring is not in equilibrium an internal force inside the rod is applied on the disks that is proportional to the difference between L and L^{rest}. This force is applied in such a way that L is pushed to L^{rest}. The internal spring force is given by

$$\mathbf{F}_{\text{int}} = -k_{\text{int}} \frac{\mathbf{L}}{L}(L^{\text{rest}} - L), \tag{2.4}$$

where k_{int} is the spring constant. By controlling the variable k_{int}, we can make sure that the distance between the disks will not deviate too much from the rest length of the spring. The ratio between D and L is called the aspect ratio, AR. In this paper AR is defined as

$$AR = \frac{L}{D}. \tag{2.5}$$

So in the case that AR is zero the rod-shaped particles and the disk-shaped particles are the same. In this thesis rods with different values for AR are examined.

2.3.2 Interaction

In the previous chapter, we discussed that the potential is nonzero when the particles start to overlap. However we have not discussed how we define an overlap. For disks an overlap means that the distance between the centre of masses of the two particles is smaller than the diameter of the disk, D. For rods however, the definition of an overlap needs more explanation. As described earlier, a rod is made up of two disks that are connected with each other by a spring force. Although the rods are made up of two connected disks, they need to interact with other rods as stadium-shaped particles (two-dimensional representation of a spherocylinder). Two overlapping rod-shaped particles are visualised in figure 3. Therefore, a function is used that computes the shortest distance from a line-segment of the first particle to the line-segment of the second particle, as is described in Ericson[11] (this was implemented by the daily supervisor

of this thesis, Meike Bos). This function returns the size, position and direction of the overlap vector **d** of this particle. d replaces then r^{ij} in the equations of the potentials above.

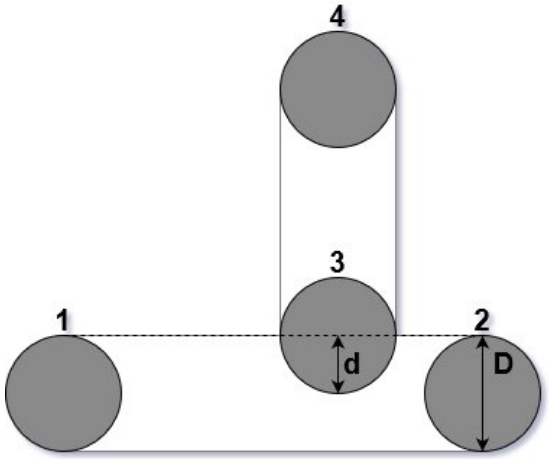

Figure 3: Two rod- shaped particles overlap each other.

2.3.3 Duplication

For the disks we used a growing mass technique. The simulation starts with one single disk, which is given some initial mass (initial mass = 0.5 in this thesis). The mass will then grow each time step by a fixed amount, while the size of the disk remains the same. If the mass comes above a critical value, c_{critical}, ($c_{\text{critical}} = 1.0$ in the simulations, so that the mass is always a value between 0.5 and 1.0) then the disk starts to duplicate itself in such a way that the two new disks have the same size but have half the mass of their mother disk.
In this simulation we used two different methods for the direction of the duplication. What we mean with the direction of the duplication, is that in the first step of the duplication procedure a new daughter disk has to appear. The mother disk is placed at the original position of the disk before the duplication starts, the daughter disk is placed a small distance away from this disk. The duplication direction is the direction the daughter disk is placed with respect to the mother disk. The mother and daughter disk only interact with each other with a strong internal spring force. This original direction is important because this dominant force will then push these disks away from each other along the direction of the vector connecting these two disks. The spring force for two different disks is given by

$$\mathbf{F}_{\text{spr}}(r) = \begin{cases} -k\dfrac{\mathbf{r}}{r}(r-D) & \text{if } r \leq D \\ \mathbf{0}, & \text{otherwise} \end{cases}$$

where D is the diameter of the disks. When the two disks are not overlapping anymore, the spring force will disappear and the two disks will interact with each other as two independent disks.
In this thesis we investigated two different duplication direction techniques. In the first method, the duplication takes place in a random direction. This means that the new emerging disk has a deviation from its original disk in a random direction. In the second method, the duplication

takes place in the y-direction. To avoid that all disks duplicate at exactly the same time we introduce a small random fluctuation in the duplication time for each particle.

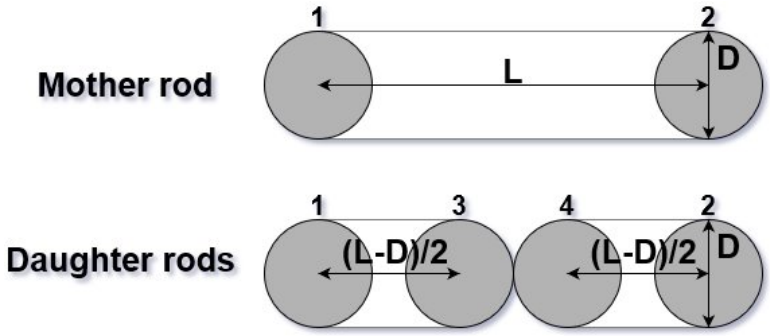

Figure 4: The mother rod particle duplicates itself by creating two new disks. The two new disks combine themselves with one of the already existing disks to form a new rod particle. This picture is inspired by [9].

For rod- shaped particles we can increase the length of the rod by just increasing L^{rest}. Here we increased L^{rest} by a fixed amount every time step. The rod particle will grow until it exceed a maximum length L_{max}. When this happens the rod particle will split into two equal parts that have both half the length of the original rod particle. This duplication is done by creating two new daughter disks between the two original parent disks. This situation is visualised in figure 4. As can be seen in the sketch, both of the mother disks are connected with a spring potential with the nearest daughter disk and form together a new rod particle, as is described in [9]. The equilibrium length of the springs of these two new rods is equal to $L^{\text{rest}}_{\text{New Rod}} = (L^{\text{rest}}_{\text{int}} - D)/2$. These new rod shaped particles will grow as independent particles until they reach the division length and divide as well.

2.4 Analysis

To analyse the simulations of the growing bacterial colonies the mean radius and the shape of the colonies have been analysed. Moreover, for the rod-shaped bacteria we also examined the nematic order parameter. These different analysis techniques are explained in more detail below.

2.4.1 Mean Radius

The mean radius has been calculated by summing up all the absolute values of the radius vectors relative to the centre of mass of the system and dividing this by the total number of particles. This is given by

$$\overline{R} = \frac{1}{N}\sum_{i=1}^{N} R_i, \tag{2.6}$$

where $R_i = |\mathbf{r}_i - \mathbf{r}_{\text{cm}}|$ is the radius of a particle with respect to the centre of mass, $\mathbf{r}_{\text{cm}} = \frac{1}{m_{\text{total}}}\sum_{i=1}^{N}\mathbf{r}_i m_i$ is the position of the centre of mass of the system and $m_{\text{total}} = \sum_i^N m_i$ is the total mass of the system. All these values have been calculated each time step.

2.4.2 Axial Ratio

To analyse the shape of the bacterial colony, we calculated the two eigenvalues and eigenvectors of the radius of gyration tensor of the colony in 2D. The 2×2 radius-of-gyration tensor is calculated relative to the centre of mass of the system for every time step. Its elements are given by

$$I_{kl} = \sum_{i=1}^{N} (||\mathbf{r}||^2 \delta_{kl} - x_k x_l). \tag{2.7}$$

Here k and l are equal to 1 and 2 respectively for the x and y coordinate. The two eigenvalues and eigenvectors are derived. The eigenvectors $\mathbf{e}_{\max}$ and $\mathbf{e}_{\min}$ give information about the direction of the longest and shortest axis of the system. The eigenvalues $\lambda_{\max}$ and $\lambda_{\min}$ give the corresponding lengths of these axis. The situation is visualised in figure 5, where the colony has an elliptical shape.

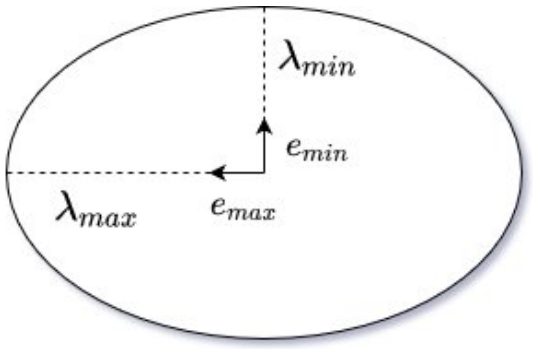

Figure 5: Vector $\mathbf{e}_{\max}$ points into the direction of the longest axis. The size of this axis is given by $\lambda_{\max}$. $\mathbf{e}_{\min}$ is the vector standing perpendicular on $\mathbf{e}_{\max}$ and the corresponding axis has a length $\lambda_{\min}$.

The axial ratio AxR is given by dividing the length of the longer axis by the length of the shorter axis. This corresponds to dividing the larger eigenvalue by the smaller one: $AxR = \frac{\lambda_{\max}}{\lambda_{\min}}$. If $AxR = 1$, we can conclude that the colony has a circular shape, whereas for $AxR \gg 1$ the shape is elliptical.

2.4.3 Nematic Order Parameter

The nematic order parameter is given by

$$S = \frac{1}{2} \langle 3 \cos(\theta_i)^2 - 1 \rangle, \tag{2.8}$$

where θ_i is the angle that the direction of rod i makes with the unit vector $\mathbf{n}$ that is named the director. This is clarified in figure 6.

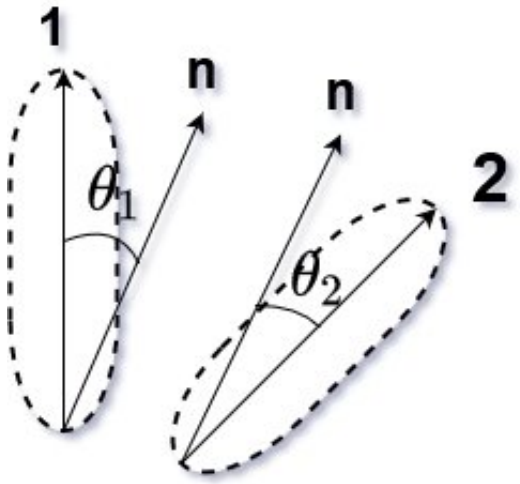

Figure 6: A sketch of two rods and the director vector. Rods 1 and 2 make an angle of θ_1 and θ_2 with the director vector respectively.

The director is equal to the average bacterial orientation. If all the rods are aligned in the same direction, then S will be equal to one, which means that the colony is in a perfect nematic state. However, if the order parameter is zero then the colony of rod-shaped bacteria does not have a preferred direction, this is called the isotropic state. The orientation of the unit vector **n** is derived by calculating the orientation of the eigenvector corresponding to the largest eigenvalue of the nematic order tensor, Q [12]. The values of the 2x2 matrix Q are given by

$$S^{kl} = \frac{1}{N}\sum_{i=1}^{N}\frac{3(u_i^k u_i^l - I^{kl})}{2}, \tag{2.9}$$

where u_i^k is the k'th component of the orientation vector of rod i and I is the 2×2 identity matrix.

3 Validation

Monte Carlo simulations give similar results as Brownian dynamics in equilibrium systems. So to check if the algorithm of the Brownian dynamics simulation is implemented correctly, we first built a Monte Carlo simulation consisting of disks that interact with each other with an Hertzian potential. For this system the expected phases are known [8] and have been used for validation of our Monte Carlo model. Afterwards, we used our Monte Carlo Simulation to validate the Brownian dynamics simulation.

3.1 Monte Carlo Simulation

The Monte Carlo Simulation is implemented for a system of fixed particle number N, volume V and a temperature T. For such an NVT ensemble the partition function is given by

$$Q = c \int d\mathbf{p}^N d\mathbf{r}^N \exp[-\mathcal{H}(\mathbf{r}^N, \mathbf{p}^N)/k_B T]. \tag{3.1}$$

Here $\mathbf{r}^N$ are the two dimensional coordinates of the system, $\mathbf{p}^N$ are the corresponding momenta, $\mathcal{H}(\mathbf{r}^N, \mathbf{p}^N)$ is the Hamiltonian of the system and c is a normalisation [13]. The probability of visiting a particular point, $\mathbf{r}^N$, is then equal to the Boltzmann factor, $\exp[-\beta U(\mathbf{r}^N)]$, where $U(\mathbf{r}^N)$ is the total potential energy of the system and $\beta = 1/k_B T$. In Monte Carlo simulations we are interested in the equilibrium state of the NVT ensemble. Therefore we can adjust the system a little bit in such a way that the system is more likely to enter a lower energy state than entering a higher energy state. This is done using the algorithm as described by Frenkel et al.[13]. Starting from a configuration state the Monte Carlo Method uses the following three steps. First, we select a particle at random and we measure its energy. Then we give the particle a random displacement. Finally, we accept this new position with a probability equal to $\min(1, \exp(-\beta[U_{new} - U_{old}]))$. This is achieved by drawing a random number between 0 and 1 and if it is smaller than this probability then the displacement is accepted.

3.2 Model

To give the Monte Carlo simulation enough time to reach the minimum energy state, we ran the simulation for 10.000 Monte Carlo steps. Moreover, periodic boundary conditions are used. So if a particle leaves the box on the left side then it will enter the box on the right side. All the simulations are done in two dimensions. The particle diameter D is used as a length scale. Furthermore, $\beta\epsilon = 1000$ and a total particle number $N = 289$. To compare the Brownian dynamics simulation with the Monte Carlo simulations we ran the simulations for different densities ρ and analysed if the shape of the crystals is the same for both simulations and are also in agreement with the findings of Fomin et al.[8]. The analysis is done by visualising the equilibrium configuration state for each simulation.

3.3 Results

The equilibrium configurations for both the Brownian dynamics simulations and the Monte Carlo simulations for $D^2\rho/m = 2.8$ and $D^2\rho/m = 3.4$ are given in figure 7. We see for both the simulations similar results: for $D^2\rho/m = 2.8$ a square crystal, see figures 7a and 7b for the Brownian dynamics and the Monte Carlo respectively. And for $D^2\rho/m = 3.4$ a dodecagonal crystal, see figures 7*c* and 7d. These crystal shapes are in agreement with the results of [8]. Therefore, we conclude that the Brownian dynamic algorithm is implemented correctly and that we can trust the outcome of the simulations.

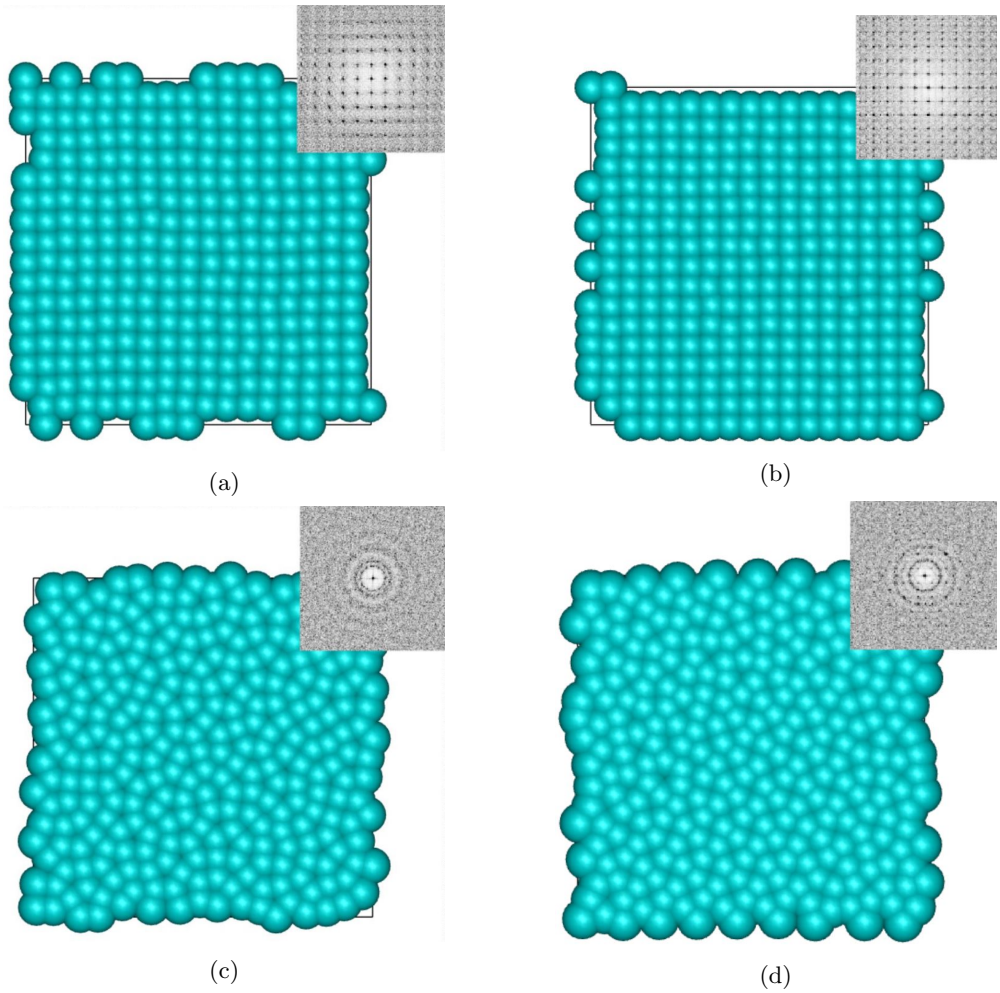

(a) (b) (c) (d)

Figure 7: (a) Brownian dynamics simulation at $D^2\rho/m = 2.8$ and $\beta\epsilon = 1000$, (b) Monte Carlo simulation at $D^2\rho/m = 2.8$ and $\beta\epsilon = 1000$, (c) Brownian dynamics simulation at $D^2\rho/m = 3.4$ and $\beta\epsilon = 1000$ and (d) Monte Carlo simulation at $D^2\rho/m = 3.4$ and $\beta\epsilon = 1000$.

4 Bacteria

The system is simulated in two dimensions. The box-sizes are set large enough so that particles never reach the end of a box. Hence, periodic boundary conditions have not to be taken into account. For every simulation 12 duplication periods are simulated. Starting with one particle at $t = 0$, this corresponds to 4096 particles at the end of the simulation. The time step that is used for disk- shaped bacteria is $\Delta t = 0.01$ and a bacterial growth $G_{\text{disks}} = 0.0005$ mass unit per Δt. Therefore, a bacteria duplicates itself in approximately 1000 steps. Furthermore, the simulation is run for 12.500 time steps, friction coefficient $\gamma = 3\pi$ and $\beta\epsilon = 1000$. For the simulations with the rods the time step and friction coefficient are the same: $\Delta t = 0.01$ and $\gamma = 3\pi$. Furthermore, the bacterial Length growth $G_{\text{rods}} = 0.0001D$ per Δt, so that a bacteria grows with one D in 10.000 time steps. Further, $\beta k_{ov} = 1000$. The simulation is run for three different aspect ratios, namely $AR = 2.0$, $AR = 3.5$ and $AR = 5.0$. The corresponding total time steps to create 12 duplication periods are respectively 200.000, 300.000 and 400.000.

4.1 Diffusion duplication ratio

The diffusion coefficient, D_{diff}, in Brownian dynamics for a two dimensional system is given by

$$D_{\text{diff}} = \frac{1}{\gamma\beta}. \tag{4.1}$$

The units of the diffusion coefficient are $\frac{[length^2]}{[time]}$. To get a time scale t_{diff} for our system we can divide a certain squared length by the diffusion coefficient. For this length we used the length that a system consisting of one particle grows in one duplication. We give this length the symbol, $L_{\text{duplication}}$. Then we get the following formula for t_{diff}

$$t_{\text{diff}} = \frac{L^2_{\text{duplication}}}{D_{\text{diff}}}. \tag{4.2}$$

So t_{diff} is the time that one particle needs to diffuse a duplication length. To study the difference between systems that are diffusion dominated or growth dominated we introduce the diffusion duplication ratio DDR. Therefore, we divide the diffusion time with the duplication time of the system. Then this dimensionless ratio DDR is given by

$$DDR = \frac{t_{\text{diff}}}{t_{\text{growth}}}. \tag{4.3}$$

If $DDR > 1$ then the duplication dominates the dynamics of a system consisting of one particle. While for $DDR < 1$ the diffusion rate dominates. For disks we used a duplication length $L_{\text{duplication}} = D$. This is because after one duplication a new disk is produced with a diameter of one D. This takes 1000 simulation steps and therefore t_{growth} for disks is $1000\Delta t$. If a rod-shaped particle duplicates it has an initial length of $\frac{L-D}{2}$, where L is equal to one of the three different aspect ratios. To grow to the new duplication period, it has to grow to L, see figure 4. Therefore, we used the difference between these two values as the duplication length for the rod-shaped particles, so $L_{\text{duplication}} = \frac{L+D}{2}$. For $AR = 2.0$, $AR = 3.5$ and $AR = 5.0$ we used $t_{\text{growth}} = 15.000\Delta t$, $t_{\text{growth}} = 22.500\Delta t$ and $t_{\text{growth}} = 30.000\Delta t$ respectively. These numbers are derived from the duplication length $L_{\text{duplication}}$ and by taking into account that a rod grows one D in 10.000 time steps.

4.2 Standard errors

To get accurate results and to find an expression for the error bars, all the simulations in this thesis have been run $n = 10$ times. In this way all the important quantities, Y can be derived by taking an average over all the runs

$$Y = \frac{1}{n}\sum_{i=1}^{n} Y_i. \tag{4.4}$$

The standard errors are then given by

$$\sigma_Y = \sqrt{\frac{1}{n-1}\sum_{i=1}^{n}(Y - Y_i)^2}. \tag{4.5}$$

For some variables Y, we plotted the logarithm function of this quantity, $\log(Y)$. In this case the error bars are derived by using the first order Taylor expansion of this function. This means that the standard deviation is given by

$$\sigma_{\log(Y)} = \frac{\sigma_Y}{Y}. \tag{4.6}$$

In this thesis different systems have be compared with each other. For the disk-shaped bacteria, systems with different duplication directions (random or fixed) and different diffusion duplication ratios are studied. For the rod-shaped bacteria different aspect ratios and different diffusion duplication ratios are analysed.

5 Results

In this chapter the results of the simulation are presented and discussed. This chapter starts with the analysis of the disk-shaped bacteria. Afterwards, the rod-shaped bacteria are investigated. Throughout this chapter different snapshots and figures are presented.

5.1 Disks

We start by analysing the results of the simulations consisting of disk-shaped particles. First, some snapshots are presented of a growing bacterial colony. Secondly, we look how the growth process depends on the duplication direction. Finally, different values of the diffusion duplication ratio are investigated.

5.1.1 Snapshots

In figure 8 different snapshots are presented of two different growing bacterial colonies consisting of disk-shaped particles. On the left side it is shown for a random duplication direction and on the right side for a fixed duplication direction. If we compare the two systems (figure 8a and 8b) after 5 duplication periods we see that the system with the fixed duplication direction (8b) has a more elliptical shape while the system with the random duplication direction has a circular shape. As the colony grows, we see that the shape of the system with the random duplication direction stays circular, see figures 8c and 8f, while the simulation with the fixed duplication direction goes from an elliptical shape to a more circular shape in figure 8d and to an almost perfectly circular shape in figure 8e. When we compare the two snapshots at the bottom we see that after 11 duplication periods the systems look very similar.

5.1.2 Colony growth as a function of the duplication direction

For the disk-shaped bacteria, the logarithm of the mean radius is plotted as a function of the duplication periods for both the systems with the random duplication direction as the systems with the fixed duplication direction with $DDR = 9.4$, as is shown in figure 9. Because $\log(\overline{R})$ grows approximately linear in time, we can conclude that the mean radius grows exponentially in time. We see that for the first few duplications the mean radius increases stepwise, but for larger duplications, around a duplication period of 8, the growth rate of the mean radius becomes more continuous. This is true for both the simulations where the growth rate is in a random direction and for the simulations where the growth rate is in a fixed direction. This can be explained by the large value of DDR, which tells us that the growth of the colony is mainly caused by the duplication rate. This means that most part of the colonial growth is created during a duplication period. However, around a duplication period of 8 this stepwise growth vanishes. This can be explained by the time it takes the system to adjust to the new state. This time increases for a larger colony size as it takes more time for the bacteria that are created at the centre to push all the other bacteria radially outward. Another explanation is the random restriction that was introduced in the duplication period of a particle.

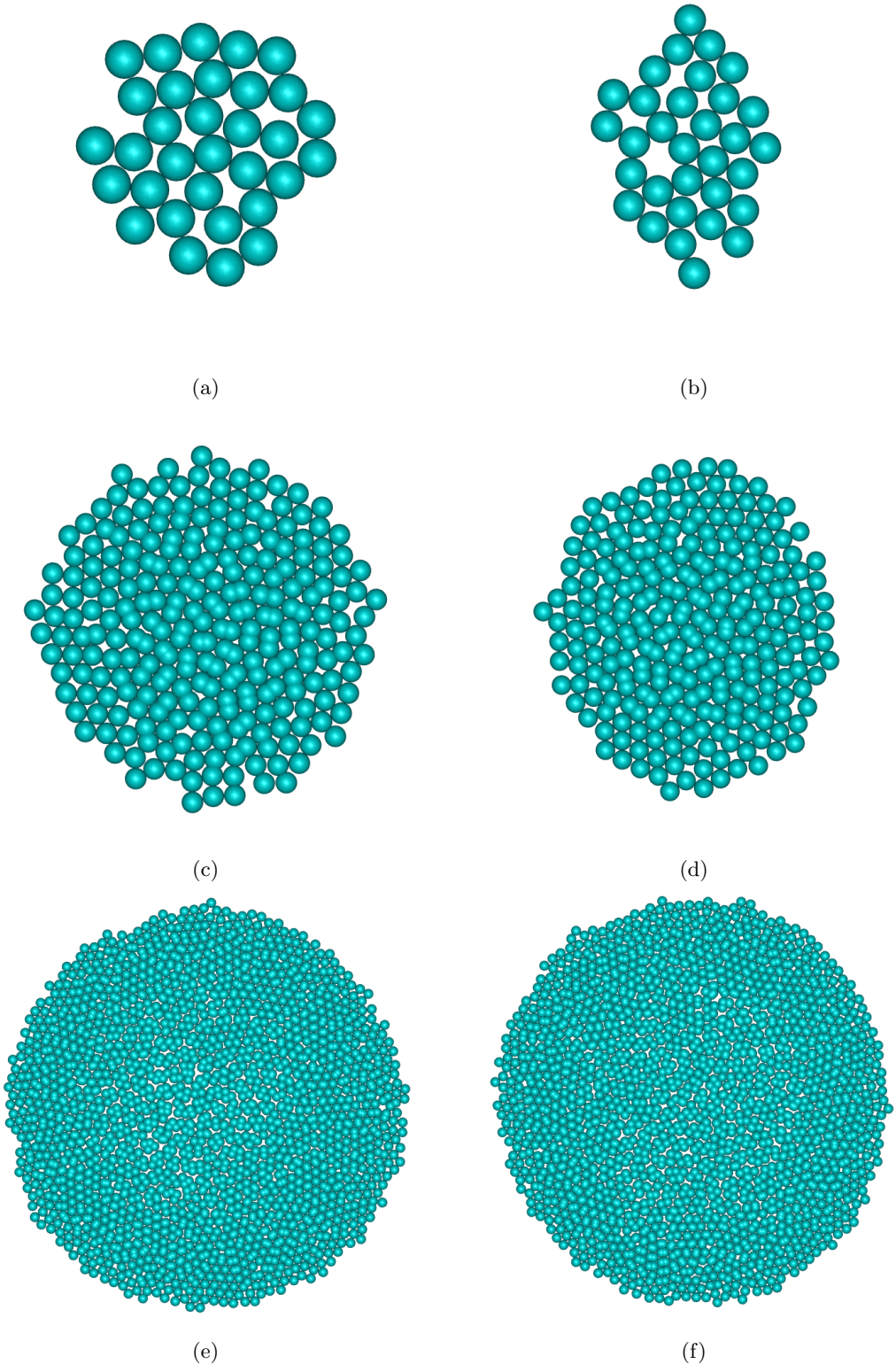

(a) (b)

(c) (d)

(e) (f)

Figure 8: Snapshots of two different disk-shaped growing bacterial colonies for random (left) and fixed (right) duplication direction. For 5 (top row), 8 (middle row) and 11 (bottom row) duplication periods.

Further, it can be noticed that $\log(\overline{R})$ of the bacterial colony that grows in a fixed direction grows faster in the first few duplication periods, but after 6 duplications they start to give similar results as the colony with the random duplication direction. On longer timescales we can conclude that the mean radius of the colony does not depend on the duplication direction, as also observed in the snapshots of the system (figure 8).

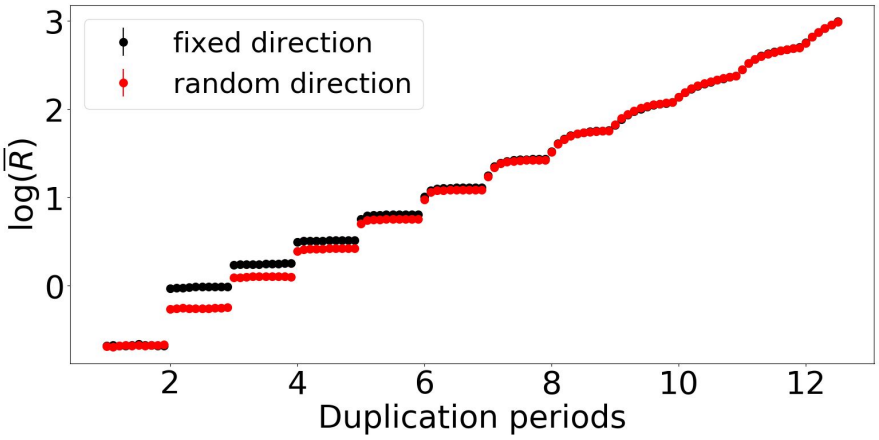

Figure 9: The logarithm of the mean radius is plotted as a function of the duplication period for disk-like bacteria with duplications in a fixed direction (black) and random direction (red).

In addition to the mean radius we also investigated the shape of the bacterial colony. In figure 10 the logarithm of the ratios of the two eigenvalues of the radius of gyration tensor, named $\log(AxR)$, are plotted as a function of the duplication periods. This has been done for both the simulations with a random duplication direction and for the simulations with a fixed duplication direction. On the logarithmic scale a value of 0 indicates a circular shape, whereas $\log(AxR) > 0$ indicates a stretched shape. For the random duplication direction we see that the logarithm of the axial ratio starts around a value of 1 and hence the shape of the colony is stretched. The reason for this is that it takes the colony some time to generate enough particles to create a circle shape. You can not create a smooth circle with a handful of disks, as can be seen in figure 8a. On a longer timescale the colony converges to a more spherical shape and after 8 duplications the colony is almost completely circular. For the fixed duplication direction the colony is far more stretched. This is due to the fact that the bacteria only duplicates itself in one direction so that a bias in a certain direction is created. After some time the pressure pushes the bacteria into the second dimension and the colony gets a more circular shape. The pressure increases even more as the colony evolves and more bacteria pop-up. Around 12 duplication periods the pressure dominates the duplication direction completely and the shape becomes circular as is the case for the system with the random duplication direction.

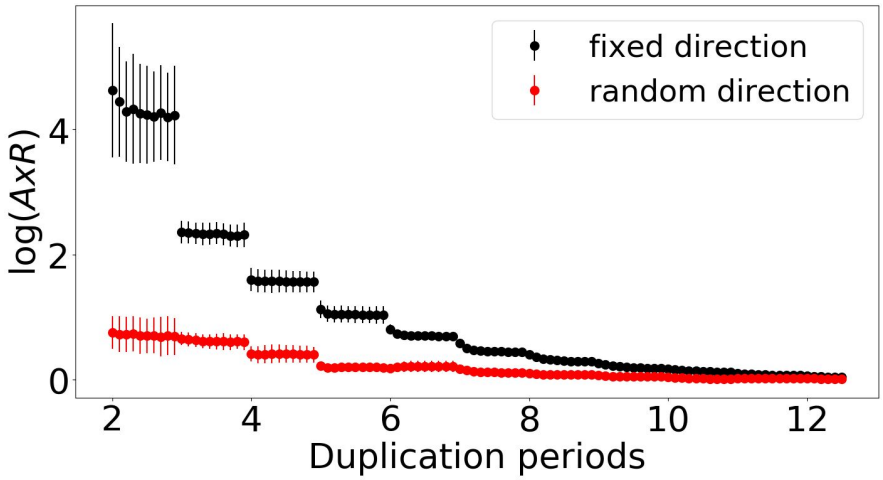

Figure 10: Plot of the logarithm of the axial ratio as a function of the duplication period for disk-like bacteria with duplications in a fixed direction (black) and random direction (red).

5.1.3 Diffusion duplication ratio

The behaviour of bacterial colonies at different diffusion duplication ratios was also studied. We used the bacterial colony with the random duplication direction. In figure 11 the logarithm of the mean radius is plotted as a function of the duplication period for different values of DDR. It shows that the mean radius increases for an decreasing DDR. However we see that for $DDR = 9.4 * 10^{-1}$ and $DDR = 9.4 * 10^{-2}$ the simulations give similar results but for $DDR = 9.4 * 10^{-3}$ and especially for $DDR = 9.4 * 10^{-4}$ the simulations generate a much greater mean radius. Further, the figure shows that for $DDR = 9.4 * 10^{-4}$ and $DDR = 9.4 * 10^{-3}$ the standard errors are larger. This can be explained by the low number of the DDR, which means that the dynamics of the system is largely governed by the diffusion rate. Then the random thermal force that create the diffusion causes the large fluctuations. On the long term however, the simulations for all the different DDR values converge to each other. The reason behind this is that the duplication rate grows exponentially fast. For the derivation of the DDR, we just took one particle into account: how much time does one particle need to diffuse one duplication length. However, as the number of particles in the system increases, the duplication rate increases as well. The simulation with $DDR = 9.4 * 10^{-2}$ converge around 7 duplication periods and the simulation with $DDR = 9.4 * 10^{-3}$ around 10 duplication periods. Furthermore, we see that the simulation corresponding to $DDR = 9.4 * 10^{-4}$ also comes close to the other three simulations at around 12 duplication periods. We find the reason why the duplication rate dominates the diffusion rate on a long timescale if we assume that the shape of the colony is circular (which is always the case on a long time scale as we saw in figure 9). After each duplication the total surface of this circle increases with a factor of two. This means that the radius of the circle increases with a factor of $\sqrt{2} \approx 1.41$. This factor is larger than one and therefore the radius is growing with an exponential rate. This explains why the duplication rate catches up with the diffusion rate.

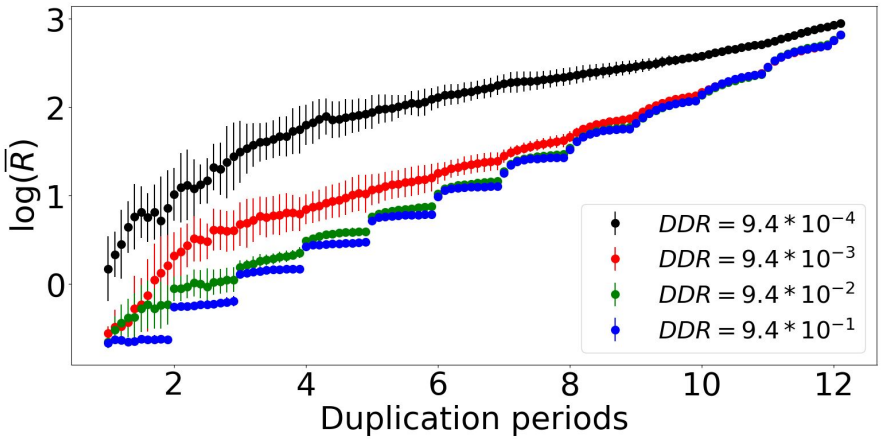

Figure 11: Disk-shaped particles with a random duplication direction. The logarithm of the mean radius is plotted as a function of the duplication period for four different diffusion duplication ratios. These are $DDR = 9.4 * 10^{-4}$ (black), $DDR = 9.4 * 10^{-3}$ (red), $DDR = 9.4 * 10^{-2}$ (green) and $DDR = 9.4 * 10^{-1}$ (blue).

5.2 Rods

Here we discuss the results of the simulations with the rod-shaped bacteria. First we present some snapshots of a growing bacterial colony, then we show how the growing colony depends on the aspect ratio. Finally, we look how different values of the diffusion duplication ratio affects the growth rate of the colony.

5.2.1 Snapshots

Snapshots of a rod-shaped bacterial colony with $AR = 5.0$ are shown in figure 12. These snapshots show that the colony grows in a similar way as the disked-shaped bacteria with a duplication in a fixed direction. In figure 12a we see that the colony is growing mostly in one dimension. Then after some time due to an increasing pressure, the colony starts to expand in the second dimension, as can be seen in figure 12b. In figure 12c the colony has already a much more circular shape, though it is still a little bit stretched. In the last figure 12d the colony is almost perfectly circular.
Another characteristic of this growing colony system is how the different rods align themselves with each other. In figure 12a the rods are well aligned and thus in a nematic state. This explains why the colony starts to grow in one direction as is the case for the disked-shaped bacteria with a fixed duplication direction. In the second figure 12b, some rods starts to get a slightly different orientation. This is due to the random thermal fluctuations and interactions of different particles. In the third figure 12c we see that the colony overall is isotropic, but on a smaller scale there are a lot of nematic subregions. The colony is now expanding in all directions and this creates the circular shape in figure 12d.

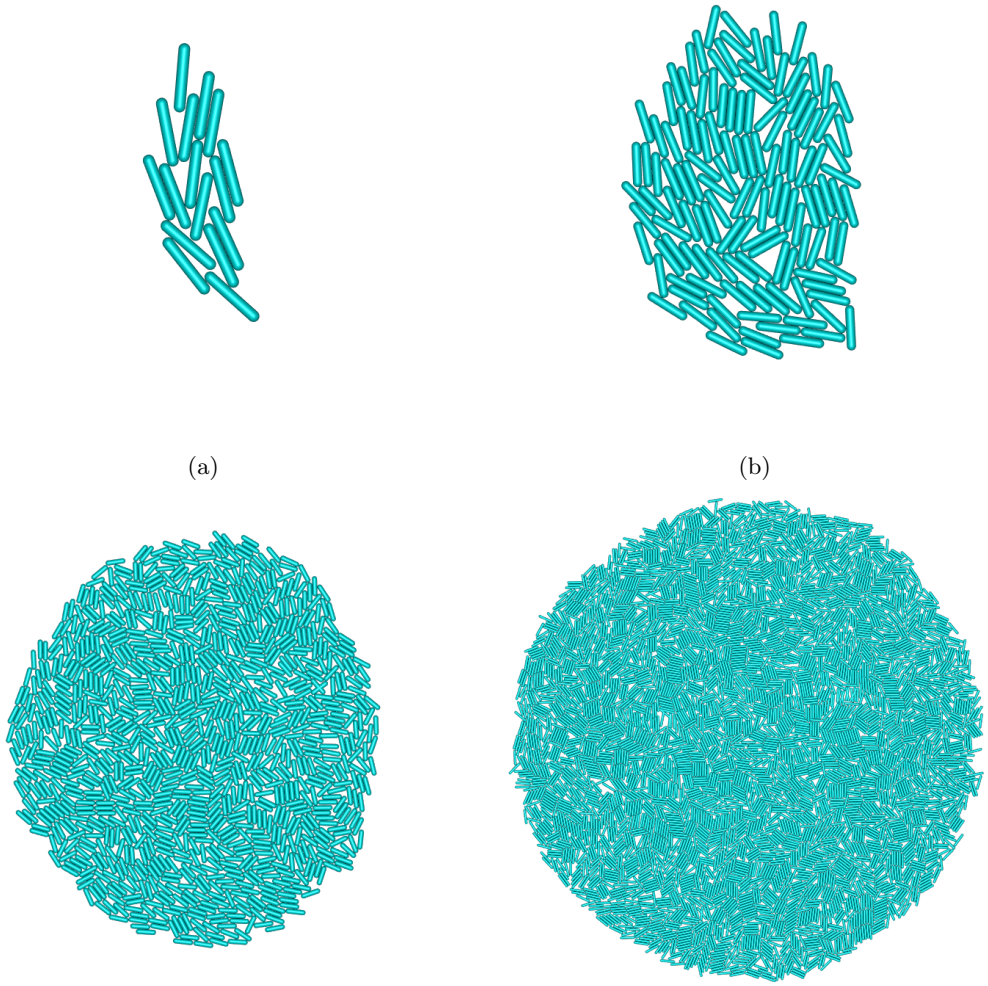

Figure 12: Four different snapshots of a rod-shaped growing bacterial colony with $AR = 5.0$. The snapshots are shown for 4, 7, 10 and 12 duplication periods for (a), (b), (c) and (d) respectively.

5.2.2 Colony growth as a function of the aspect ratio

In figure 13 the logarithm of the mean radius is plotted as a function of the duplication periods for three different aspect ratios. These are $AR = 2.0$, $AR = 3.5$ and $AR = 5.0$. Again an exponential growth rate can be observed for all three rod-sized particles as $\log(\overline{R})$ grows linearly in time. At around 2 duplication periods we see a peak for $AR = 3.5$ and $AR = 5.0$. The reason for this is that the mean radius is calculated by averaging over all the positions of the disks in the system relative to the centre of mass. If the two rods duplicate to four rods, then four new disks are created that are positioned relatively close the centre of mass. Therefore, the two disks that are positioned farthest away from the centre of mass receive a smaller weight and the mean radius declines. Furthermore, the figure shows that a higher aspect ratio leads to a larger colony size. This is due to the fact that rods with a higher aspect ratio have also a

larger surface area.

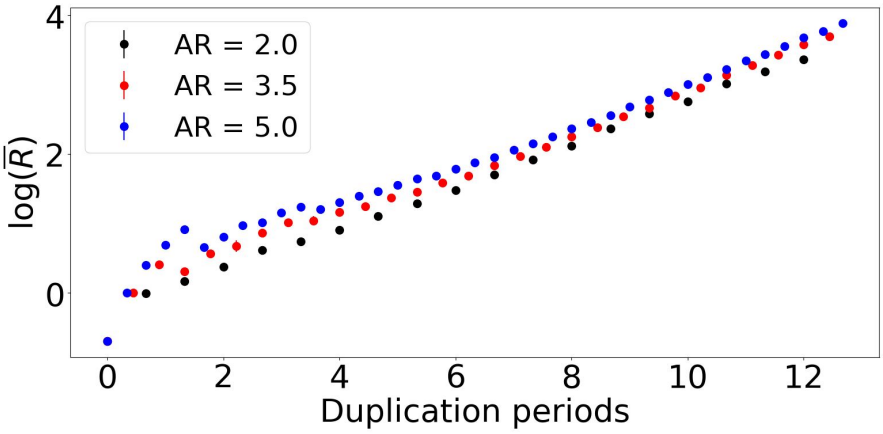

Figure 13: The logarithm of the mean radius is plotted a function of the duplication period for three different aspect ratios. These are particles with $AR = 2.0$, $AR = 3.5$ and $AR = 5.0$ corresponding to the black, red and blue dots respectively.

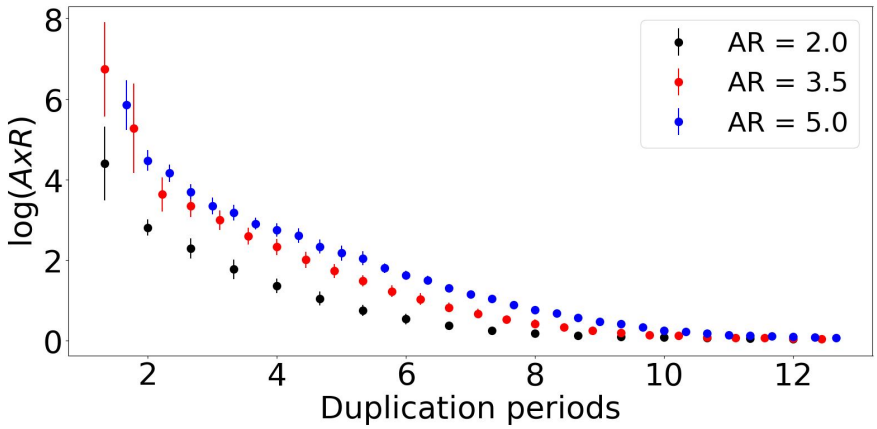

Figure 14: The logarithm of the axial ratio is plotted as a function of the duplication period for three different aspect ratios. These are particles with $AR = 2.0$, $AR = 3.5$ and $AR = 5.0$ corresponding to the black, red and blue dots respectively.

From the snapshots of figure 12 we noticed that in the first time steps the colony has an elliptical shape and that this shape transformed to a circular shape later in time. This is in agreement with figure 14 where the axial ratio on a logarithmic scale is plotted against the duplication periods for the three different aspect ratios. $\log(AxR) = 0$ indicates again a circular shape and $\log(AxR) > 0$ a stretched shape. The figure shows that the ratio converges from a stretched start state to a circular end state for all the three aspect ratios. Moreover, bacteria with a higher aspect ratio converge significantly slower than bacteria with a smaller aspect ratio. This indicates that the rods with a higher aspect ratio are more aligned than the rods with a lower

aspect ratio, since rods only grow in the direction of their orientation. To further explore this behaviour, we will now look to the results of the nematic order parameter.

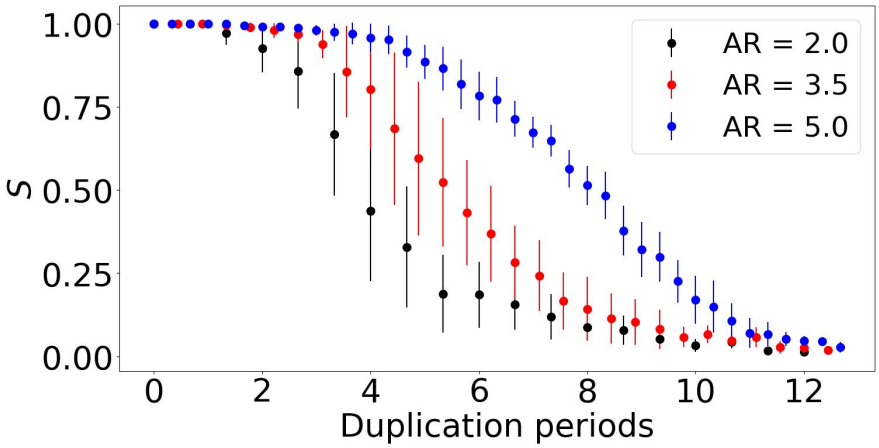

Figure 15: The order parameter is plotted as a function of the duplication period for three different aspect ratios. These are $AR = 2.0$, $AR = 3.5$ and $AR = 5.0$ corresponding to the black, red and blue dots respectively.

The nematic order parameter is plotted as a function of the duplication direction in figure 15. In agreement with the previous results, the bacterial colonies with the higher aspect ratio tends to be more aligned than the bacteria with a smaller aspect ratio, as is shown in figure 15. The reason for this is that it is harder for particles with a large aspect ratio than for particles with a small aspect ratio to push another particle away. Therefore it is more efficient for a bacteria to align itself besides its neighbour and when it gets on that position, it gets locked up by its neighbours so that it is difficult for the particle to move away. Figure 15 confirms this by showing that the simulations with a small aspect ratio ($AR = 2.0$) converges much faster to zero than the larger sized rods. Although the larger particles with an aspect ratio of 5.0 tend to align better, at larger timescales the overall orientation disappears. The colony as a whole falls into a large number of sub nematic regions that are all orientated in another direction so that the colony as a whole behaves in a more isotropic way, as can be seen by the snapshots of 12.

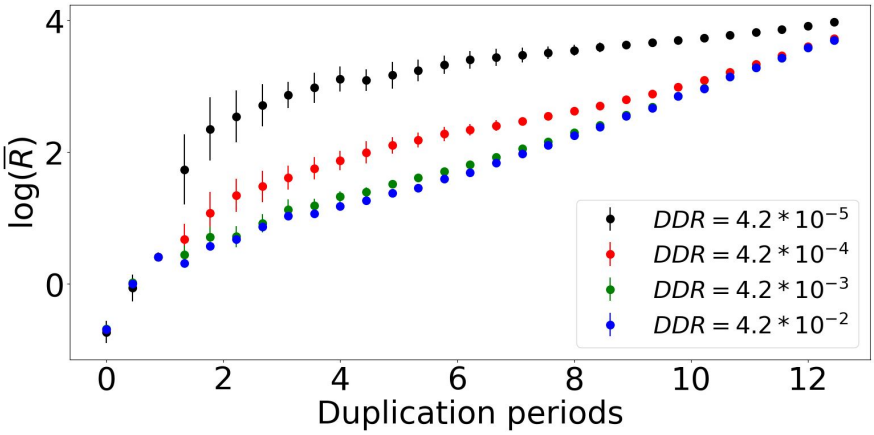

Figure 16: The mean radius is plotted as a function of the duplication period for four different temperatures. These are $\beta = 0.1$, $\beta = 1$, $\beta = 10$ and $\beta = 100$ corresponding to the black, red, green and blue dots respectively.

5.2.3 Diffusion duplication ratio

We analyse the effect of the diffusion duplication ratio for rod-shaped particles with an aspect ratio of 3.5. This is done by plotting the logarithm of the mean radius as a function of the duplication periods for four different values of DDR. These are $DDR = 4.2 * 10^{-5}$, $DDR = 4.2 * 10^{-4}$, $DDR = 4.2 * 10^{-3}$ and $DDR = 4.2 * 10^{-2}$. The results are presented in figure 16. We see that the sizes of the colony for the different values of DDR start at 0 and that on a long time scale they all converge. However, in between these two limits we see that the simulations with a lower value of DDR have a larger size than the colonies with a higher value of DDR. This is a result of the diffusion of the particles caused by the thermal motion. A lower value of DDR means a higher diffusion rate. For $DDR = 4.2 * 10^{-5}$, $DDR = 4.2 * 10^{-4}$ and $DDR = 4.2 * 10^{-3}$ this diffusion is the main driving force for the first few duplication periods. However, as can be seen in figure 13 the colony is growing exponentially. So after some time the exponential growth rate of the system catches up the movements of the diffusion and the colony becomes a liquid crystal with nematic subregions. This process is shown in more detail by the snapshots in figure 17 with $DDR = 4.2 * 10^{-4}$. In the first two snapshots, see figures 17a and 17b, the diffusion dominates the dynamics of the system. This means that a particle on average has enough time to diffuse away before it get pushed by the other particles in the colony. As the bacteria keep duplicating themselves the particles will have less free space and starts to interact with neighbouring particles, see figure 17c. In figure 17d the diffusion rate is not large enough and the dynamics of the particles is mostly caused by the growing colony that pushes all the other particles radially outward.

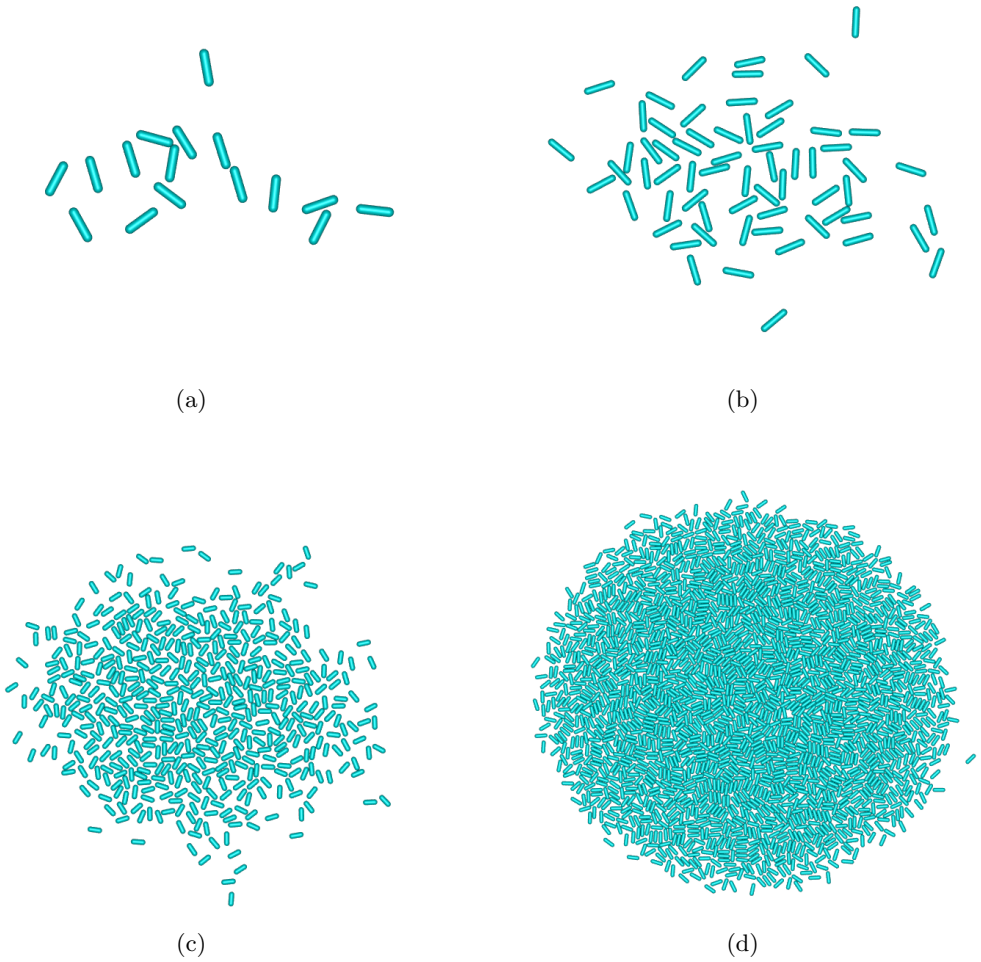

(a) (b)

(c) (d)

Figure 17: Four different snapshots of a rod-shaped growing bacterial colony with $AR = 3.5$ and $DDR = 4.2 * 10^{-4}$. The snapshots are shown for 4, 6, 9 and 11 duplication periods for (a), (b), (c) and (d) respectively.

6 Discussion

In this thesis we modeled nonmotile bacterial colonies for different aspect ratios and different diffusion rates. The behaviour of the bacteria are simulated using Brownian dynamics. We ignored inertial effects in this model because the system has a low Reynolds number. The Reynolds number is much smaller than one for bacteria in a viscous fluid, due to the small sizes of the bacteria cells, they have a diameter in the order of a few micrometers. This is known as an overdamped system. We implemented our rod-shaped bacteria in the same way as was done by Nordemann et al.[9]. Rod-shaped bacteria are modeled as spherocylinders formed by connecting two disks with a spring force. Furthermore, the particles are made soft so that an overlap results in a repulsive force. This seems reasonable because bacteria deform under pressure. In the paper they also used an overdamped system and therefore we would expect similar results.

In this thesis, we found that a rod-shaped bacterial colony converge over time to a circular state with nematic subregions. This is in agreement with Nordemann et al.[9], where they also found that over time a bacterium system becomes round with distinct regions of aligned particles. Just as in the paper we also analysed the nematic order parameter S as a function of the aspect ratio. We found similar results. Over time S goes to 0, so that on average the bacteria have not a preferred orientation and S goes faster to zero for a lower aspect ratio. Therefore we concluded that our model is implemented correctly.

In this thesis, we also added new contributions to this model. We compared the disk- and rod-shaped simulations with each other and we concluded that the disk-shaped particles with a fixed duplication direction have similar characteristics as the rod-shaped particles: they start with an elliptical shape and end in a circular shape. For the disk-shaped particles the transformation from an elliptical to a circular shape is only caused due to the outward radial pressure. Therefore, we concluded that the transformation to a circular shape of rod-shaped bacterial colonies is not solely a result of the nematic alignments of the bacteria, but more a consequence of the radially outward pressure. However the creation of disorder, that switches the nematic orientation of the system to an isotropic orientation, is speeding up this process. For a nematic orientation the rods all grow in a fixed direction (like the disks with a fixed duplication direction), whereas for an isotropic orientation the rods grow into all directions (like the disks with a random duplication direction). As we have seen for the disk-shaped particles, a random duplication direction creates a circular shape on all timescales. So the sooner a rod-shaped bacterial colony becomes isotropic, the sooner it starts to behave like a disk-shaped bacterial colony with a random duplication direction and a circular shape. So what we conclude is that on a long timescale all the studied bacterial colonies becomes circular due to inner pressure and that the formation of disorder can speed up this process for a rod-shaped bacterial colony. Furthermore, we analysed how the diffusion duplication ratio DDR affects the growth of the colony. If we look for lower DDR values then we concluded that on a short time scale the diffusion rate dominates the dynamics of the system. This is indicated by a higher value of the mean radius of the colony. However, on a longer timescale the mean radius of the colony converges to the mean radius of a colony with a higher value of DDR. The reason for this is that as the colony grows in time, the exponentially growing duplication rate will eventually become larger than the diffusion rate and all the particles will be caught up by the expanding colony.

In this thesis we made the assumption that the particles grow a fixed amount per time step. Disks grow with a fixed mass unit, while rods grow a fixed length unit per time step. This is of

course not really realistic as bacteria only grow when there is food in the system. As the colony grows, a high density region at the center is created. So especially in this region food will be scarce and it is unlikely that these bacteria grow at the same rate as the bacteria on the outer regions of the colony. In further research it is a good idea to take this into account. Furthermore, we saw the creation of nematic subregions that have not been given much attention in this thesis. Therefore it would be interesting to study the structure in the colony on a local scale. In the simulations we also looked to an isolated system, consisting of just one bacteria at $t = 0$. In real life situations it is however likely that there are more colonies growing and colliding with each other. These colonies could consist of bacteria with different shapes. Therefore it is an idea to run the current simulations for a polydisperse system. So instead of starting with one particle in the initial state, we could start with multiple particles of different aspect ratios. In this way we could analyse the interaction of different shaped bacterial colonies with one another.

7 Conclusion

In this thesis we simulated and investigated two different growing bacterial colonies. One consisting of disk-shaped particles and one consisting of rod-shaped particles. The dynamics of the system are implemented using Brownian dynamics with a spring potential. We analysed the systems by using three different measurements. We looked at the mean radius, the shape of the colony and the nematic order parameter, where the latter one is just used for the rod-shaped particles. The analysis were done with a high value of the diffusion duplication ratio DDR so that the duplication rate dominated the dynamics of the system. Therefore we used $DDR = 9.4$ for disks and $DDR = 4.2 * 10^{-1}$ for rods. For the disk-shaped particles we investigated how the duplication direction (random or fixed) affects the colony and for the rod-shaped particles we analysed how the aspect ratio ($AR = 2.0$, $AR = 3.5$ and $AR = 5.0$) influences the properties of the system. Moreover, we studied how the colony size depends on higher diffusion rates by comparing simulations with lower values of DDR. For disks we compared systems with $DDR = 9.4 * 10^{-1}$, $DDR = 9.4 * 10^{-2}$, $DDR = 9.4 * 10^{-3}$ and $DDR = 9.4 * 10^{-4}$. For rods we analysed $DDR = 4.2 * 10^{-2}$, $DDR = 4.2 * 10^{-3}$, $DDR = 4.2 * 10^{-4}$ and $DDR = 4.2 * 10^{-5}$.

For the disk-shaped simulations, this thesis concludes that a growing bacterial colony has a growth rate that increases exponentially in time. On a short timescale this growth rate is larger for the disks with a fixed duplication direction and the shape of the colony is stretched in the average duplication direction. This includes an elliptical shape for the fixed duplication direction and a circular shape for the random direction. On a longer timescale the duplication direction does not affect the shape nor the growth rate of the system and the shape becomes circular expanding in all directions at the same speed. For rod-shaped particles we found an exponentially growth rate. Furthermore, on a short timescale the system is in a nematic state where all the particles have a similar orientation. Because rods grow in the direction of their orientation, this produces an elliptical shape. However, on the long run disorder is created due to inner pressure and thermal motion. This results to a circular isotropic global state consisting of nematic subregions. Moreover, this thesis showed that the number of duplication periods in which the colony reaches the isotropic state increases for a higher aspect ratio. This means that disorder is more easily formed for particles with a lower aspect ratio than for particles with a higher aspect ratio. Furthermore, we analysed how an increasing diffusion rate affects the growth process of disk- and rod-shaped bacterial colonies. We found on a short timescale that a higher diffusion rate creates a disordered state with a higher mean radius, whereas on a longer timescale the duplication rate dominates the dynamics of the system so that the systems with different diffusion rates look the same.

This thesis made the assumption that bacteria always grow a fixed amount per time step. However, bacteria only grow if they have enough food. Food will be scarce at the center of the colony and therefore the assumption that all the bacteria grow with the same amount is not realistic. In future work, it is therefore an idea to relax on this restriction. Furthermore a polydisperse system, consisting of both rod-and disk shaped bacteria, can also be investigated.

References

[1] Sriram Ramaswamy. "The mechanics and statistics of active matter". In: *Annu. Rev. Condens. Matter Phys.* 1.1 (2010), pp. 323–345.

[2] Andrea Cavagna and Irene Giardina. "Bird flocks as condensed matter". In: *Annu. Rev. Condens. Matter Phys.* 5.1 (2014), pp. 183–207.

[3] Christopher M Waters and Bonnie L Bassler. "Quorum sensing: cell-to-cell communication in bacteria". In: *Annu. Rev. Cell Dev. Biol.* 21 (2005), pp. 319–346.

[4] HoJung Cho, Henrik Jönsson, Kyle Campbell, Pontus Melke, Joshua W Williams, Bruno Jedynak, Ann M Stevens, Alex Groisman, and Andre Levchenko. "Self-organization in high-density bacterial colonies: efficient crowd control". In: *PLoS biology* 5.11 (2007).

[5] PDG Wilson, TF Brocklehurst, S Arino, D Thuault, M Jakobsen, Martin Lange, J Farkas, JWT Wimpenny, and JF Van Impe. "Modelling microbial growth in structured foods: towards a unified approach". In: *International journal of food microbiology* 73.2-3 (2002), pp. 275–289.

[6] Zell A McGee, David S Stephens, Loren H Hoffman, Walter F Schlech III, and Robert G Horn. "Mechanisms of mucosal invasion by pathogenic Neisseria". In: *Reviews of infectious diseases* 5.Supplement_4 (1983), S708–S714.

[7] HU Bertschinger and J Pohlenz. "Bacterial colonization and morphology of the intestine in porcine Escherichia coli enterotoxemia (edema disease)". In: *Veterinary pathology* 20.1 (1983), pp. 99–110.

[8] Yu D Fomin, EA Gaiduk, EN Tsiok, and VN Ryzhov. "The phase diagram and melting scenarios of two-dimensional Hertzian spheres". In: *Molecular Physics* 116.21-22 (2018), pp. 3258–3270.

[9] Gerhard Nordemann, Martijn Wehrens, Sander Tans, Timon Idema, et al. "Defect dynamics in growing bacterial colonies". In: *arXiv preprint arXiv:2003.10509* (2020).

[10] Tomas Storck, Cristian Picioreanu, Bernardino Virdis, and Damien J Batstone. "Variable cell morphology approach for individual-based modeling of microbial communities". In: *Biophysical journal* 106.9 (2014), pp. 2037–2048.

[11] Christer Ericson. *Real-time collision detection*. CRC Press, 2004.

[12] Daan Frenkel. "Statistical mechanics of liquid crystals". In: *les Houches* (1991), pp. 689–762.

[13] Daan Frenkel and Berend Smit. "Molecular dynamics simulations". In: *Understanding Molecular Simulation* 2 (2002), pp. 63–107.